



Published in final edited form as:

Kidney Int. 2016 June ; 89(6): 1281–1292. doi:10.1016/j.kint.2016.01.030.

Endostatin and transglutaminase 2 are involved in fibrosis of the aging kidney

Chi Hua Sarah Lin¹, Jun Chen¹, Zhongtao Zhang², Gail Johnson³, Arthur JL Cooper², Julianne Feola³, Alexander Bank¹, Jonathan Shein¹, Heli Ruotsalainen⁴, Taina Pihlajaniemi⁴, and Michael S Goligorsky¹

¹Departments of Medicine, Pharmacology and Physiology, Renal Research Institute ²Department of Biochemistry, New York Medical College, Valhalla, NY ³Department of Anesthesiology, University of Rochester, Rochester, NY ⁴Oulu Center for Cell-Matrix Research, Biocenter Oulu and Faculty of Biochemistry and Molecular Medicine, University of Oulu, Finland

Abstract

Endostatin (EST), an anti-angiogenic factor, is enriched in aging kidneys. EST is also an interactive partner of transglutaminase 2 (TG2), an enzyme that cross-links extracellular matrix proteins. Here we tested whether EST and TG2 play a role in the fibrosis of aging. In wild type mice, aging kidneys exhibited a 2–4 fold increase in TG2 paralleled by increased cross-linked extracellular matrix proteins and fibrosis. Mice transgenic to express EST showed renal fibrosis at a young age. One month delivery of EST via minipumps to young mice showed increased renal fibrosis that became more robust when superimposed on folic acid-induced nephropathy. Upregulated TG2 and impaired renal function were apparent with EST delivery combined with folic acid-induced nephropathy. Subcapsular injection of TG2 and/or EST into kidneys of young mice not only induced interstitial fibrosis, but also increased the proportion of senescent cells. Thus, kidney fibrosis in aging may represent a natural outcome of upregulated EST and TG2, but more likely it appears to be a result of cumulative stresses occurring on the background of synergistically acting geronic (aging) proteins, EST and TG2.

Keywords

aging kidney; endostatin; collagen 18; tissue transglutaminase; fibrosis

Address correspondence to: Michael_goligorsky@nymc.edu.

Disclosure

Authors declare that they have nothing to disclose

Publisher's Disclaimer: This is a PDF file of an unedited manuscript that has been accepted for publication. As a service to our customers we are providing this early version of the manuscript. The manuscript will undergo copyediting, typesetting, and review of the resulting proof before it is published in its final citable form. Please note that during the production process errors may be discovered which could affect the content, and all legal disclaimers that apply to the journal pertain.

INTRODUCTION

Microvascular rarefaction is a constant companion of nephrosclerosis developing in the aging kidney. Forty years of studies of angiogenesis and its endogenous inhibitors have yielded a long list of endogenous molecular mediators, some of which are used as therapeutics to enhance or suppress vascular growth and consequently modulate structure and function of organs involved. Endostatin (EST), the pleiotropic anti-angiogenic factor, is one of such mediators. It is a 20–22 kDa C-terminal fragment of collagen XVIII¹, generated by the action of proteases, such as matrix metalloproteinases (–3,–7,–9,–13,–14, and –20)². Collagen XVIII is a ubiquitous component of basement membranes especially in vessels with fenestrated endothelium, like those in renal glomeruli and peritubular capillaries^{3–5}. In our recent studies, we have demonstrated that the levels of EST are significantly elevated in the blood and tissues of aging mice, specifically in the kidney⁶. We have also demonstrated that this elevation was associated with impairment of peritubular capillary patency, but have not provided definitive proof in regard to whether EST alone is sufficient to trigger renal interstitial fibrosis. Notably, the most recently published clinical study links elevation in EST level with kidney injury in the elderly patients⁷.

Tissue transglutaminase (TG2), a recently identified molecular partner of EST⁸, is a multifunctional protein richly expressed on the surface of vascular endothelium and in the extracellular matrix, where it interacts with fibronectin, collagen, osteopontin, heparin, and syndecan-4^{9–10}. The two main functions of TG2 on the cell surface and in the interstitium are catalysis of Ca²⁺ dependent cross-linking reaction of ECM proteins to stabilize extracellular matrix (ECM) by forming covalent γ -glutamyl-N^ε-lysine bond between acyl donor and acyl acceptor and scaffolding for cell adhesion¹¹. TG2 has been shown to participate in fibrotic processes: inhibition of TG2 reduces tubulointerstitial fibrosis and preserves function in experimental chronic kidney disease models^{12–14} and decreases pulmonary fibrosis¹⁵. Physiologic consequences of its partnership with EST have not been previously investigated and the precise mechanism of how EST and TG2 interact to regulate fibrosis remains unknown. Therefore, in the present studies we sought to elucidate the mutual dynamics and pathogenic role of these two pro-fibrogenic proteins, EST and TG-2, and the possibility of their synergistic action in aging kidney. To meet the requirements for functioning as geronic proteins, TG2 and EST have to be a) present in excess in aging animals and b) be able to induce upon their overexpression signs of aging in young animals. These criteria were investigated herein.

RESULTS

Expression of TG2 in aging mouse kidneys

Analysis of TG2 expression in kidneys obtained from aging mice (C57 strain) revealed that the level was increased 2–4-fold compared to young animals (Fig 1, A). The increased TG2 was located in extracellular space as demonstrated by immunofluorescence staining (Fig 1, B). To assess whether the changes in the cross-linking activity parallel the increased expression of TG2 in aging kidneys, we analyzed the level of γ -glutamyl-N^ε-lysine, in young and aging kidneys. TG2-induced cross-linking product γ -glutamyl-N^ε-lysine was significantly elevated in aging kidneys (Fig 1, C), thus confirming that TG2 in aging mice

was also enzymatically active. Moreover, γ -glutamyl-N^ε-lysine was increased in extracellular area of aging kidney.

Western blot analysis of aging kidneys revealed 2 bands (Fig 1, A). The molecular weight of full length TG2 is 75kDa, however, the molecular weight for TG2 fragment increased in the aging mice detected on WB was ~ 53kDa. The detection of two bands immunoreactive with antibodies against TG2 suggests a proteolytic cleavage of TG2. Other investigators showed that cell surface TG2 can be cleaved predominantly by MT1-MMP (matrix metalloproteinase 14, MMP-14) at Pro-375, Arg-458 and His-461 to produce ~53kDa, ~41kDa and ~32kDa proteolytic fragments in a process that regulates cell locomotion¹⁶ and mineralization¹⁷, regardless of its cross-linking activity. Thus, we examined the expression of the MMP-14 and found it to be also increased in aging kidneys (Fig 2, A). For that reason, we examined in vitro the possible involvement of MMP-14 in this process. Indeed, co-incubation of recombinant TG2 with conditioned medium obtained from 293T cells transfected with the plasmid containing human MMP-14 extracellular domain revealed a second smaller (~53kDa) band immunoreactive with TG2 antibody, indicating that MMP-14 is able to cleave TG2. (Fig 2, B). Furthermore, both ~75kDa TG2 and ~53kDa fragment of TG2 were not detectable in the kidneys obtained from TG2^{-/-}, used as a negative control, as demonstrated by WB. This indicates that ~53kDa fragment is derived from TG2 (Fig 2, C). Although the enzymatic activity of this fragment of TG2 has not been studied in detail (technical problems related to the loss of the tertiary structure of the enzyme prevented the use of the hydroxamine assay for detection of its activity), the very fact of significantly elevated cross-linking product γ -glutamyl-N^ε-lysine in the aging kidney (Fig 1, C) suggests that it possesses an increased cross-linking activity.

Role of TG2 in angiogenesis

In order to address the question of the role of TG2 in fibrosis of aging, we performed a series of in vitro studies. Conflicting studies have proposed that extracellular TG2 crosslinking activity either inhibits or stimulates angiogenesis¹⁸⁻¹⁹. In our angiogenesis competence experiments conducted with matrigel-embedded aortic rings we observed, as in the previous studies²⁰⁻²¹, a robust sprouting of endothelial cells forming capillary-like structures (Fig 3, A). When matrigel was pretreated with two different concentrations of TG2 prior to embedding of aortic rings, capillary sprouting was dose-dependently suppressed (Fig 3, A). One of the possible causes for such suppression could be attributed to the resistance of TG2 cross-linked extracellular matrix proteins to proteolytic degradation, the necessary component of angiogenesis. Indeed, when we examined the “halo” phenomenon, a result of matrixolytic activity, the disappearance of the matrixolytic zone around aortic rings showed a dose-dependent decline with the increasing concentration of TG2 (Fig 3, B). Collectively, these findings suggest that the elevated levels of TG2 could be responsible for the observed fibrosis and microvascular rarefaction in aging kidneys, as previously reported⁶.

Studies on overexpression of TG2 in the kidney

We next considered overexpressing TG2 in the kidney. We injected TG2 into intact kidneys of 3 months old C57BL/6 mice. In preliminary studies, we ensured that a small amount of

injection, 10 μ l, is sufficient to diffuse throughout the kidney. We used 1% Evans blue dye as a color marker injected directly into lower pole and observed a very rapid (within a few minutes) discoloration of one fourth area of the kidney (Supplementary Fig 1, A). Kidney vessels and interstitial areas were all stained with Evans blue dye 24 hours after injection (Supplementary Fig 1, B). Next, we injected TG2 at the concentration of 1 μ g in 10 μ l volume (this concentration was selected after an extensive preliminary testing of cross-linking capacity). Forty-eight hours later, kidneys displayed enhanced γ -glutamyl-N^e-lysine immunofluorescence (Supplementary Fig 1, C). The data demonstrate that elevated levels of TG2 alone can be contributory to enhanced matrix fibers cross-linking, a step preceding accumulation of poorly degradable collagens and fibronectin. When similarly treated kidneys were examined 14 days post-injection of TG2 in combination with 2 μ g EST, this resulted in increased interstitial fibrosis (Fig 4, A).

Overexpression of EST and its role in TG2 expression and fibrosis

In order to examine possible EST contribution to interstitial fibrosis and TG2 expression, we used EST transgenic mice (EST-tg). EST-tg mice have a 7-fold increase in EST level in the circulation²². Data presented in Fig 4, B revealed that matrix deposition in the tubulointerstitium of kidneys of EST-tg mice was significantly increased already at a young age, 2–3 months-old. This elevation was further enhanced by the age of 10–12 months. To confirm the role of EST in interstitial fibrosis of aging kidney and overcome possible problems related to the life-long EST overexpression, we implanted EST peptide-containing osmotic minipumps to young mice with or without folic acid-induced chronic nephropathy. As the duration of disease culminating in significant fibrosis requires 12 weeks, we divided our animals into six groups including control, FA-induced nephropathy alone, EST peptide minipumps alone implanted either early at the first four weeks or late after 8 weeks, EST peptide minipumps implanted at the time of FA-induced nephropathy, and EST peptide minipumps implanted late into the disease (8 weeks after the induction of nephropathy) (time-course: Fig 5, A). When EST peptide minipumps were implanted early in the course of study (E-EST group), the degree of fibrosis was elevated 2-fold (picosirius red staining) (Fig 5, B), and α -SMA immunofluorescence staining was increased 3-fold (Fig 5, C). In contrast, EST peptide minipumps implanted late into the course of study (L-EST group) failed to significantly change the degree of fibrosis compared with control. The results indicate that long-term (3 months), but not short-term elevation of EST alone is sufficient to induce accumulation of extracellular matrix protein, albeit at a moderate degree. Notably, when EST peptide minipumps were implanted early in the course of disease together with folic acid-induced nephropathy (FA/E-EST group), the degree of interstitial fibrosis was dramatically increased 11-fold (Fig 5, B) and showed a 13-fold increase in α -SMA immunofluorescence staining compared to control (Fig 5, C). Moreover, this group of mice also showed a significant microvascular rarefaction, as judged by decreased CD31 immunofluorescence staining (Fig 6)

TG2 protein (Fig 7, A) and cross-linking product γ -glutamyl-N^e-lysine level (Fig 7, B) in the extracellular matrix showed no differences in the E-EST and L-EST groups. However, TG2 expression and cross-linked extracellular matrix were significantly elevated in mice with folic acid-induced nephropathy in combination with the early implanted EST minipumps

(FA/E-EST group). Similarly, proteinuria was significantly increased in mice implanted early with EST minipumps, either with or without folic acid-induced nephropathy (FA/E-EST, E-EST and FA/L-EST groups), but was marginal in mice with the late EST minipump implantation (L-EST group) (Fig 7, C). Serum creatinine and BUN were significantly elevated in mice with folic acid-induced nephropathy implanted with EST minipumps early or late in the course of the disease (FA/E-EST and FA/L-EST) (Fig 7,D, E). The reason for a comparable elevation in FA-L-EST mice remains unknown.

Effects of EST and TG2 overexpression on cell senescence

To elucidate whether TG2 and/or EST are capable of inducing premature senescence of renal cells in young mice, 2–3 month-old mice were injected with TG2, EST, or both, as detailed previously. Senescent cells were visualized by immunofluorescence staining for senescence-associated heterochromatic foci (SAHF). The concept of SAHF was first proposed by Narita and Lowe²³. One of the markers, H3K9me3, as shown in Fig 8, A, 2 weeks after subcapsular injection of TG2 or EST into the kidneys of young mice, the proportion of heterochromatin accumulation was significantly enhanced. Paradoxically, the combination of EST with TG2 resulted in the lower proportion of senescent cells compared to each alone (Fig 8, A) This paradox was resolved by the finding that the number of in situ detected dead cells (TUNEL-positive) in fibrotic areas of the same TG2+EST combination group was significantly increased compared to each protein injected alone (Fig 8, B). Occasionally observed speckled cytoplasmic pattern of TUNEL staining in tubular epithelial cells was consistent with the previously described phagocytosis of apoptotic bodies²⁴. Moreover, when EST peptide minipumps were implanted to young mice for one month (E-EST group), the percentage of cells with SAHF was significantly elevated, as judged by the increased number of H3K9me3 stained cells (Supplementary Fig 2). Folic acid-induced nephropathy alone also significantly increased the number of senescent cells. In addition, when EST peptide minipumps were implanted in mice with folic acid-induced nephropathy (FA/E-EST group), the proportion of senescent cells was further increased to 9.4%. Collectively, data show that EST and TG2 are not only fibrogenic, but also geronic proteins.

DISCUSSION

Data presented herein show intricate relations between EST and TG2, both of which we find to be overexpressed in aging mouse kidney. A proteolytic fragment of TG2 is the predominant species accumulating in aging kidneys, but its activity is preserved judging by the fact that γ -glutamyl-N^ε-lysine cross-linking product is elevated in aging kidneys (Fig 1, C). The attempts to mimic the lack of EST or TG2 using genetically engineered mice turned to be non-informative due to multitude of other functions of those proteins, thus compounding analysis of end-points (not shown). Much more relevant to the context of these aging studies, the experiments with overexpression of each of these proteins strongly support the idea of their interactive participation in fibrosis and senescence. Moreover, the effect of overexpression of these proteins, even in young animals, is dramatically amplified by the concomitant kidney stress of folic acid-induced nephropathy, the “second hit” model. Impaired renal function, pro-fibrotic effect and premature senescence are all induced in this model.

Regarding the interaction between EST and TG2, EST binds with a low-nanomolar affinity to TG2 in the Ca²⁺ dependent manner via Arg²⁷ and Arg¹³⁹. The GTP binding site in the TG2 serves as a putative binding site for EST⁸; suggesting that EST may interact with the catalytically active form of the enzyme. Arg²⁷ and Arg¹³⁹ of the EST are also critical for alternative binding to heparin, αVβ3 and α5β1 integrins²⁵. Based on the in vitro experiments, exogenous EST is incapable of directly upregulating the expression of TG2 in cultured endothelial cells (Supplementary Fig 3). However, the states of EST overexpression in mice with EST peptide chronic minipump delivery (with and without FA-induced nephropathy), are consistently associated with upregulation of TG2 levels and enhanced TG2 cross-linking activity (Fig 7, A, B), perhaps, indicating that the EST effect is indirect and requires the input of additional messengers.

In an attempt to resolve the possibility of synergistic action of EST and TG2, we performed molecular modeling. Indeed, molecular modeling of TG2 interaction with EST sheds light on the possible synergistic effect of these two geronic proteins, as schematically depicted in Figure 9. Analysis of published studies indicates that it is very likely that EST binds to the C-terminal β-barrel domains. First, EST binding to TG2 is abolished when high concentrations of GTP is present, indicating that EST most likely binds to the buried surfaces between C domain and β-barrels as those surface areas are not accessible when TG2 is in the closed conformation upon GTP/GTP binding. Secondly, EST does not bind to the N-terminal domain of TG2, as the N-terminal domain is freely accessible either in the closed or open conformation. Thirdly, EST is neither a substrate, nor an inhibitor of TG2, indicating that EST does not bind anywhere near the catalytic site of the catalytic domain. We conducted in silico docking studies between TG2 (open conformation, 2Q3Z) and EST (1BNL) to further confirm our analysis with ZDOCK²⁶ and ClusPro²⁷ without any bias introduced. The top scorers from ZDOCK predominantly show that EST interacts with β-barrels, whereas ClusPro analysis gives complexes of EST interacting with either N-terminal domain, or β-barrels, with the latter being more consistent with above analysis. In addition, the two arginine residues R27 and R139 from EST play important roles in the interaction with TG2 in the docking model, consistent with literature reports⁸. In fact, immunoprecipitates of TG2 from native lysates prepared from mouse kidneys confirms that EST is also present in pulled down TG2 (Fig 9, D). These findings raise the following possible corollaries for the observed upregulation of EST and TG2: 1) both may be contributing to the vascular rarefaction and fibrosis in aging kidney and 2) both may be pathogenically related and their effects synergistic. It is impossible, at the present time, to distinguish which of these geronic proteins is the pathogenic driver.

Our findings also show that the expression of the master metalloproteinase, MMP-14, another enzyme cleaving collagen XVIII to release EST fragment, is upregulated in aging kidneys (Fig 2). Therefore, the possible role of MMP-14 may be complex: on the one hand, it can cleave collagen XVIII to yield EST²; on the other hand, TG2 itself is a substrate for MMP14-initiated proteolytic degradation¹⁶ potentially leading to acquisition of the active conformation of the enzyme.

Our studies establish that the excess EST alone is sufficient to induce fibrosis (Fig 4, B and Fig 5, B). Moreover, the most telling findings are those obtained using the combination of

folic acid-induced nephropathy with EST delivery via implanted minipumps. It is remarkable that EST delivery early in the course of folic acid nephropathy, at the time of acute, “wound healing” phase, has produced the most damaging results (Fig 5 and Fig 6). This phase is characterized by an intense angiogenic response and interfering with it, as in our model by chronic infusion of EST, brings about an exaggerated fibrotic response. This argument may explain why stressors are more harmful in aging animals, which regularly overexpress EST. On the other hand, delivery of EST during the chronic phase of folic acid nephropathy, does not dramatically affect its course, suggesting that effects of EST are mostly confined to angiogenic processes, when vessels are immature, but effects of EST are diminished in the mature microvasculature. This assumption would indicate that the very fact of overexpressed EST in aging kidney should have modest consequences until a nephrotoxic stressor arises. The most recent demonstration of the association between higher circulating EST levels and lower GFR and higher albuminuria in elderly individuals⁷, provides additional credence to the above murine studies.

In conclusion, our study reveals that 1) TG2 is significantly elevated in aging mice; 2) endostatin alone triggers interstitial fibrosis in both EST transgenic mice and mice with increased EST by chronic delivery for 1 month via minipumps; 3) exaggerated fibrotic response is revealed when nephropathy is induced by FA on the background of elevated endostatin level, especially during the “wound healing” phase. The increased susceptibility of aging kidneys to nephrotoxic agents has been well-documented and molecular mechanisms, including hemodynamics, oxidative stress, inflammation, apoptosis, decreased repair have been proposed²⁸. The present studies allow to conclude that kidney fibrosis in aging could be a natural outcome of unregulated EST and TG2, but also emphasize an increased likelihood of being a cumulative result of renal stresses occurring on the background of elevated geronic proteins, EST and TG2.

MATERIALS AND METHODS

Experimental animals and cultured endothelial cells

The animal study protocol was in accordance with the National Institutes of Health *Guide for the Care and Use of Laboratory Animals* and was approved by the Institutional Animal Care and Use Committee. Experiments were conducted in 3 mo-old male FVB mice divided into 6 groups: Control (DMSO) group ($n = 5$), chronic fibrotic phase of folic acid nephropathy (FA) group ($n = 3$), early-endostatin (E-EST) peptide group ($n=4$), FA+ E-EST peptide group ($n=4$), late-endostatin (L-EST) peptide group ($n=3$) and FA+ L-EST peptide group ($n=3$). In addition, kidneys of 6 mo-old and 24 mo-old C57 mice (obtained from the National Institute on Aging, Baltimore, MD) were analyzed.

Studies were also performed in transgenic mice overexpressing EST under the keratin K14 promoter (2~3 mo-old and 10~12 mo-old wild type [WT] and transgenic mice kidney samples obtained from the University of Oulu), characterized by a 7-fold increase in the circulating level of EST²². These mice show thickening of basement membranes in the skin, but their kidneys have not been studied.

Kidney samples were also obtained from the previously characterized TG2 knockout mice^{29–30} from the University of Rochester, NY (2~3 mo-old and 13~14 mo-old WT and KO mice in C57BL/6 background).

The included file, Supporting Information Materials and Methods, describes Western Blot analysis, Co-immunoprecipitation of TG2 and EST, Immunofluorescence staining, Aortic outgrowth assay, Matrigel proteolysis analysis, Injection of 1% Evans blue dye or TG2 into the kidney, Western blot analysis of TG2 fragmentation, Folic acid model of chronic progressive nephropathy, Chronic delivery of Endostatin peptide, Picrosirius Red staining, Albumin, creatinine and BUN measurements, Endothelial Cell culture, and Statistical analyses.

Supplementary Material

Refer to Web version on PubMed Central for supplementary material.

Acknowledgments

These studies were supported in part by the NIH grants DK54602, DK052783, DK45462 (MSG) and Westchester Artificial Kidney Foundation. Data presented herein were a part of Dr Lin's PhD thesis (2015). Authors are grateful to Dr J Cao (SUNY, Stony Brook, NY) for sharing the mutated MMP-14 plasmid, to David Lee for technical assistance during early phases of this work, and to Drs. Edward Lakatta and Yevgeniya Lukyanenko (Laboratory of Cardiovascular Science, National Institutes of Health, National Institute on Aging, Baltimore, MD) for providing kidneys of aged mice.

References

1. O'Reilly MS, Boehm T, Shing Y, et al. Endostatin: an endogenous inhibitor of angiogenesis and tumor growth. *Cell*. 1997; 88:277–285. [PubMed: 9008168]
2. Ferreras M, Felbor U, Lenhard T, et al. Generation and degradation of human endostatin proteins by various proteinases. *FEBS Lett*. 2000; 486:247–251. [PubMed: 11119712]
3. Marneros AG, Olsen BR. Physiological role of collagen XVIII and endostatin. *FASEB J*. 2005; 19:716–728. [PubMed: 15857886]
4. Muragaki Y, Timmons S, Griffith CM, et al. Mouse Col18a1 is expressed in a tissue-specific manner as three alternative variants and is localized in basement membrane zones. *Proc Natl Acad Sci U S A*. 1995; 92:8763–8767. [PubMed: 7568013]
5. Rehn M, Pihlajaniemi T. Alpha 1(XVIII), a collagen chain with frequent interruptions in the collagenous sequence, a distinct tissue distribution, and homology with type XV collagen. *Proc Natl Acad Sci U S A*. 1994; 91:4234–4238. [PubMed: 8183894]
6. Lin CH, Chen J, Ziman B, et al. Endostatin and kidney fibrosis in aging: a case for antagonistic pleiotropy? *Am J Physiol Heart Circ Physiol*. 2014; 306:H1692–1699. [PubMed: 24727495]
7. Ruge T, Carlsson AC, Larsson TE, et al. Endostatin Level is Associated with Kidney Injury in the Elderly: Findings from Two Community-Based Cohorts. *Am J Nephrol*. 2014; 40:417–424. [PubMed: 25401956]
8. Faye C, Inforzato A, Bignon M, et al. Transglutaminase-2: a new endostatin partner in the extracellular matrix of endothelial cells. *Biochem J*. 2010; 427:467–475. [PubMed: 20156196]
9. Gundemir S, Colak G, Tucholski J, et al. Transglutaminase 2: a molecular Swiss army knife. *Biochim Biophys Acta*. 2012; 1823:406–419. [PubMed: 22015769]
10. Belkin AM. Extracellular TG2: emerging functions and regulation. *FEBS J*. 2011; 278:4704–4716. [PubMed: 21902810]
11. Eckert RL, Kaartinen MT, Nurminskaya M, et al. Transglutaminase regulation of cell function. *Physiol Rev*. 2014; 94:383–417. [PubMed: 24692352]

12. Huang L, Haylor JL, Hau Z, et al. Transglutaminase inhibition ameliorates experimental diabetic nephropathy. *Kidney Int.* 2009; 76:383–394. [PubMed: 19553913]
13. Shweke N, Boulous N, Jouanneau C, et al. Tissue transglutaminase contributes to interstitial renal fibrosis by favoring accumulation of fibrillar collagen through TGF-beta activation and cell infiltration. *Am J Pathol.* 2008; 173:631–642. [PubMed: 18688035]
14. Johnson TS, Fisher M, Haylor JL, et al. Transglutaminase inhibition reduces fibrosis and preserves function in experimental chronic kidney disease. *J Am Soc Nephrol.* 2007; 18:3078–3088. [PubMed: 18003782]
15. Olsen KC, Sapinoro RE, Kottmann RM, et al. Transglutaminase 2 and its role in pulmonary fibrosis. *Am J Respir Crit Care Med.* 2011; 184:699–707. [PubMed: 21700912]
16. Belkin AM, Akimov SS, Zaritskaya LS, et al. Matrix-dependent proteolysis of surface transglutaminase by membrane-type metalloproteinase regulates cancer cell adhesion and locomotion. *J Biol Chem.* 2001; 276:18415–18422. [PubMed: 11278623]
17. Nakano Y, Forsprecher J, Kaartinen MT. Regulation of ATPase activity of transglutaminase 2 by MT1-MMP: implications for mineralization of MC3T3-E1 osteoblast cultures. *J Cell Physiol.* 2010; 223:260–269. [PubMed: 20049897]
18. Jones RA, Kotsakis P, Johnson TS, et al. Matrix changes induced by transglutaminase 2 lead to inhibition of angiogenesis and tumor growth. *Cell Death Differ.* 2006; 13:1442–1453. [PubMed: 16294209]
19. Wang Z, Perez M, Caja S, et al. A novel extracellular role for tissue transglutaminase in matrix-bound VEGF-mediated angiogenesis. *Cell Death Dis.* 2013; 4:e808. [PubMed: 24052076]
20. Baker M, Robinson SD, Lechertier T, et al. Use of the mouse aortic ring assay to study angiogenesis. *Nat Protoc.* 2012; 7:89–104. [PubMed: 22193302]
21. Vasko R, Xavier S, Chen J, et al. Endothelial Sirtuin 1 Deficiency Perpetrates Nephrosclerosis through Downregulation of Matrix Metalloproteinase-14: Relevance to Fibrosis of Vascular Senescence. *J Am Soc Nephrol.* 2013
22. Elamaa H, Sormunen R, Rehn M, et al. Endostatin overexpression specifically in the lens and skin leads to cataract and ultrastructural alterations in basement membranes. *Am J Pathol.* 2005; 166:221–229. [PubMed: 15632014]
23. Narita M, Nunez S, Heard E, et al. Rb-mediated heterochromatin formation and silencing of E2F target genes during cellular senescence. *Cell.* 2003; 113:703–716. [PubMed: 12809602]
24. Bedner E, Li X, Gorczyca W, et al. Analysis of apoptosis by laser scanning cytometry. *Cytometry.* 1999; 35:181–195. [PubMed: 10082299]
25. Faye C, Moreau C, Chautard E, et al. Molecular interplay between endostatin, integrins, and heparan sulfate. *J Biol Chem.* 2009; 284:22029–22040. [PubMed: 19502598]
26. Pierce BG, Wiehe K, Hwang H, et al. ZDOCK server: interactive docking prediction of protein-protein complexes and symmetric multimers. *Bioinformatics.* 2014; 30:1771–1773. [PubMed: 24532726]
27. Kozakov D, Beglov D, Bohnuud T, et al. How good is automated protein docking? *Proteins.* 2013; 81:2159–2166. [PubMed: 23996272]
28. Wang X, Bonventre JV, Parrish AR. The aging kidney: increased susceptibility to nephrotoxicity. *Int J Mol Sci.* 2014; 15:15358–15376. [PubMed: 25257519]
29. Nanda N, Iismaa SE, Owens WA, et al. Targeted inactivation of Gh/tissue transglutaminase II. *J Biol Chem.* 2001; 276:20673–20678. [PubMed: 11274171]
30. Colak G, Johnson GV. Complete transglutaminase 2 ablation results in reduced stroke volumes and astrocytes that exhibit increased survival in response to ischemia. *Neurobiol Dis.* 2012; 45:1042–1050. [PubMed: 22198379]
31. Cao J, Sato H, Takino T, et al. The C-terminal region of membrane type matrix metalloproteinase is a functional transmembrane domain required for pro-gelatinase A activation. *J Biol Chem.* 1995; 270:801–805. [PubMed: 7822314]

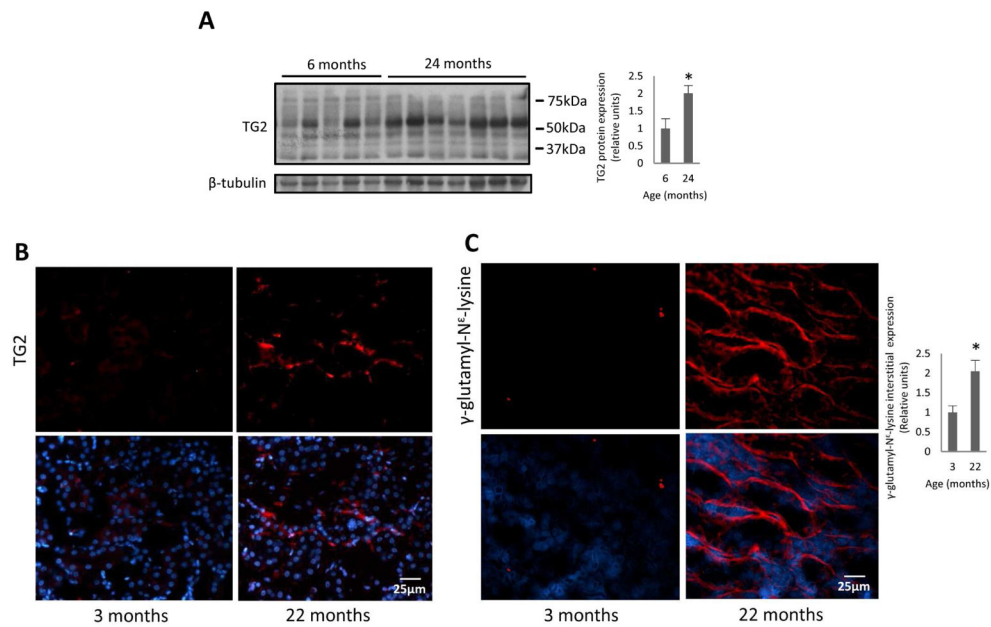


Fig 1. TG2 protein and cross-linking product γ -glutamyl-N^ε-lysine expression in aging mouse kidneys

(A) TG2 protein expression is increased in 24-months-old C57 mice as demonstrated by western blotting. Right panel: Quantification of band density using NIH image J software. n=5–7 animals per group. Note that the reported full length of TG2 molecular mass is around 75kDa. However, the molecular mass for increased TG2 in the aging mice is approximately 53kDa. (B) Representative immunohistochemical images of extracellular TG2 expression in 3 and 22-month-old C57 mice; magnification of $\times 400$. (C) TG2 cross-linking product γ -glutamyl-N^ε-lysine, was increased in 22-months-old C57 mice as demonstrated by immunofluorescence staining. Right panel: Quantification of integrated density using NIH image J software. Bottom panels depict merged images with the nuclear counterstaining. n=3 animals per group. Data are means \pm SEM. *P<0.05.

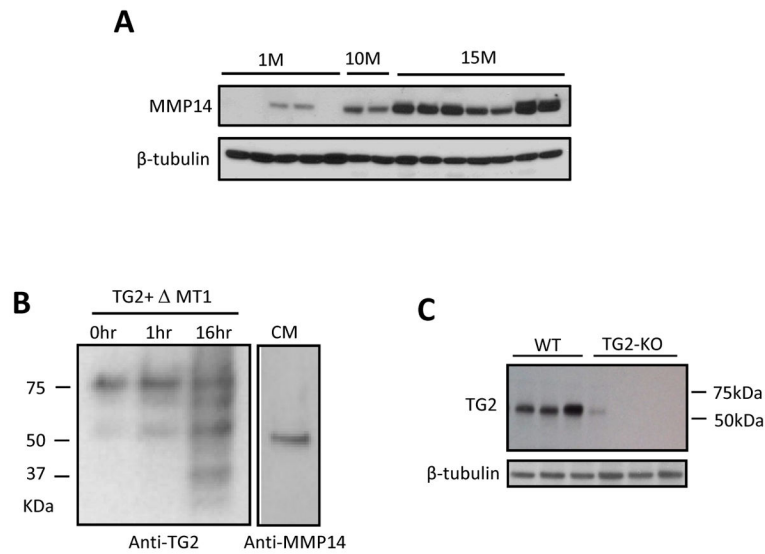


Fig 2. Analysis of TG2 fragmentation

A. MMP14 protein expression in aging kidney. Expression of MMP-14 is increased in aging mice kidneys in a time-dependent manner (FVB mouse strain). n=5 for 1-month-old, n=2 for 10 month-old, and n=7 for 15 month-old mice.

B. Western blot analysis of TG2 fragmentation: TG2 fragmentation by MMP14. TG2 from guinea pig liver (100 ng) was incubated for 0, 1, and 16 hours (lines 1, 2, and 3, respectively) in serum-free conditioned medium collected from HEK293T cells that were transfected with pcDNA- MT1 construct containing the extracellular domain of human MMP14. The products were blotted and detected with monoclonal TG2 antibody. Note that the band intensity of the smaller fragments (53kDa and 22 kDa) increases along with the duration of incubation. Lane 4 represents conditioned medium (CM) (10 ul) that was blotted with monoclonal MMP14 antibody.

C. The ~53kDa fragment is absent in TG2^{-/-} mice. Monoclonal anti-TG2 antibodies detecting multiple bands on WB in **B**. ~53 kDa fragment of TG2 were undetectable in the TG2^{-/-} kidneys. n=3 animals per group.

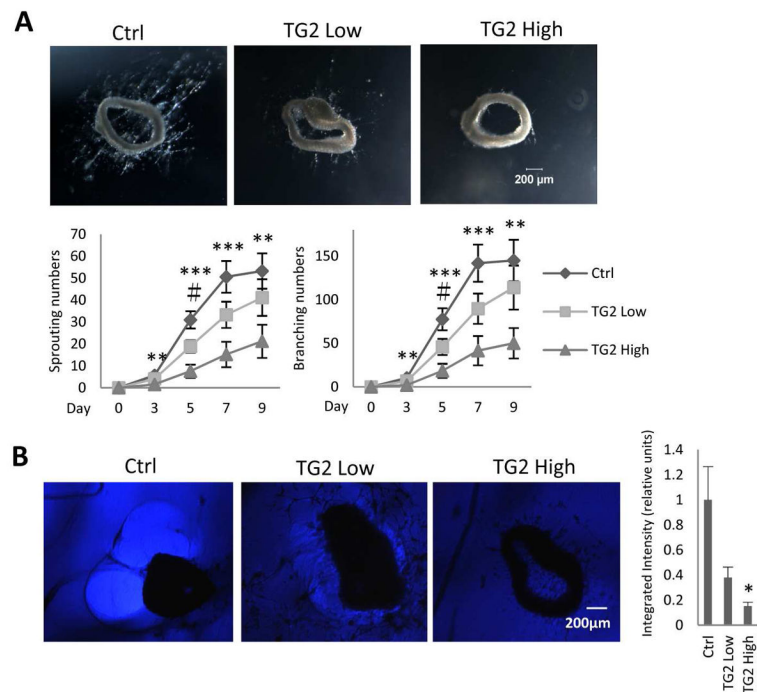


Fig 3. Effects of matrix-enriched TG2 on ex vivo angiogenesis and matrilytic activity

A. Exogenous TG2 in matrigel inhibits angiogenesis in a dose-dependent manner in an *ex vivo* mouse aorta ring assay. Aortic segments obtained from 3-months-old C57 mice were cut into 1-mm rings, embedded in Matrigel pre-treated with or without 100 ug/ml and 500 ug/ml TG2, cultured in EGM-2 culture medium for 9 days and monitored every 2 days. Sprouting and branching were counted. Top panel: Representative images at a magnification of $\times 40$. Bottom panel: The kinetics of sprouting and branching. Note that the exogenous TG2-pretreated matrigel inhibits angiogenesis in a dose-dependent manner. Both the sprouting and the branching commenced on day 3. Data are means \pm SEM. *** $P < 0.001$, ** $P < 0.01$, # $P < 0.05$, $n = 7$ each group

B. Inhibition of proteolytic degradation in a dose-dependent manner in matrigel pre-treated with TG2 in a mouse aortic assay *ex vivo*. Left panel: Broad bright “halo” formation of proteolytically degraded matrigel, a functional manifestation of MMP enzymatic activity, was consistently seen around individual cultured aortic rings. When matrigel was pre-treated with different concentrations of TG2 (100 ug/ml or 500 ug/ml), the “halo” phenomenon exhibited a dose-dependent attenuation. Right panel: Quantitative analyses of the integrated intensity using NIH image J software. Magnification of $\times 40$. Data are means \pm SEM. * $P < 0.05$, $n = 4$ each group

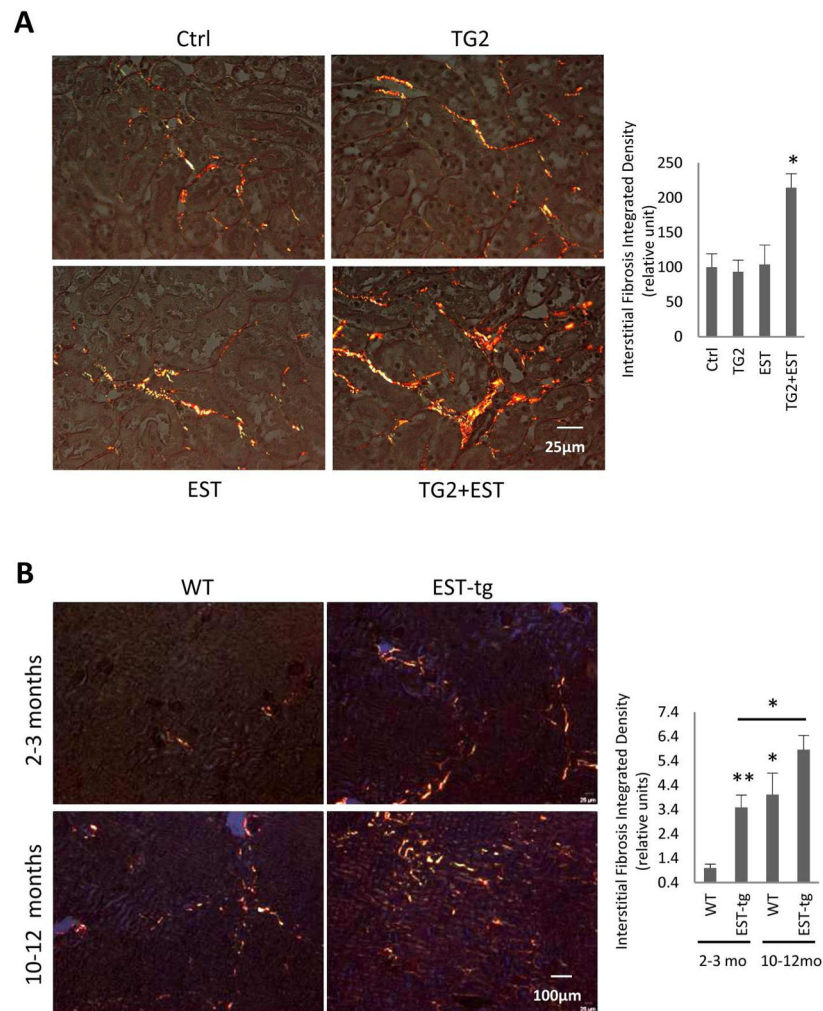


Fig 4. Increased interstitial fibrosis after overexpression of EST and TG2 by subcapsular injection into kidney

(A) Fourteen days after kidney lower pole injection either with buffer, 2ug of EST peptide, 1 ug of TG2 or a combination of TG2 and EST dissolved in 10 μ l buffer. TG2 together with EST injected mouse kidneys show increased interstitial fibrosis as analyzed by picrosirius red positive area staining. Representative images for each group are shown at magnification of $\times 400$. Right panel: Quantification of interstitial fibrosis area was performed using integrated density by Image J at $\times 100$ magnification. Data are mean \pm SEM. * $P < 0.05$, $n = 3-4$ animals per group. **(B) Interstitial fibrosis in kidneys of transgenic mice overexpressing EST.** Collagen expression is increased in the EST overexpressing mouse kidneys already at the age of 2–3 months and it is further enhanced in 10–12 months-old mice. Left panel: Representative images for each group are shown at magnification of $\times 100$. Right panel: Quantification of integrated density using NIH image J software. Magnification $\times 100$. Data are means \pm SEM. ** $P < 0.01$, * $P < 0.05$. $n = 5$ animals per group.

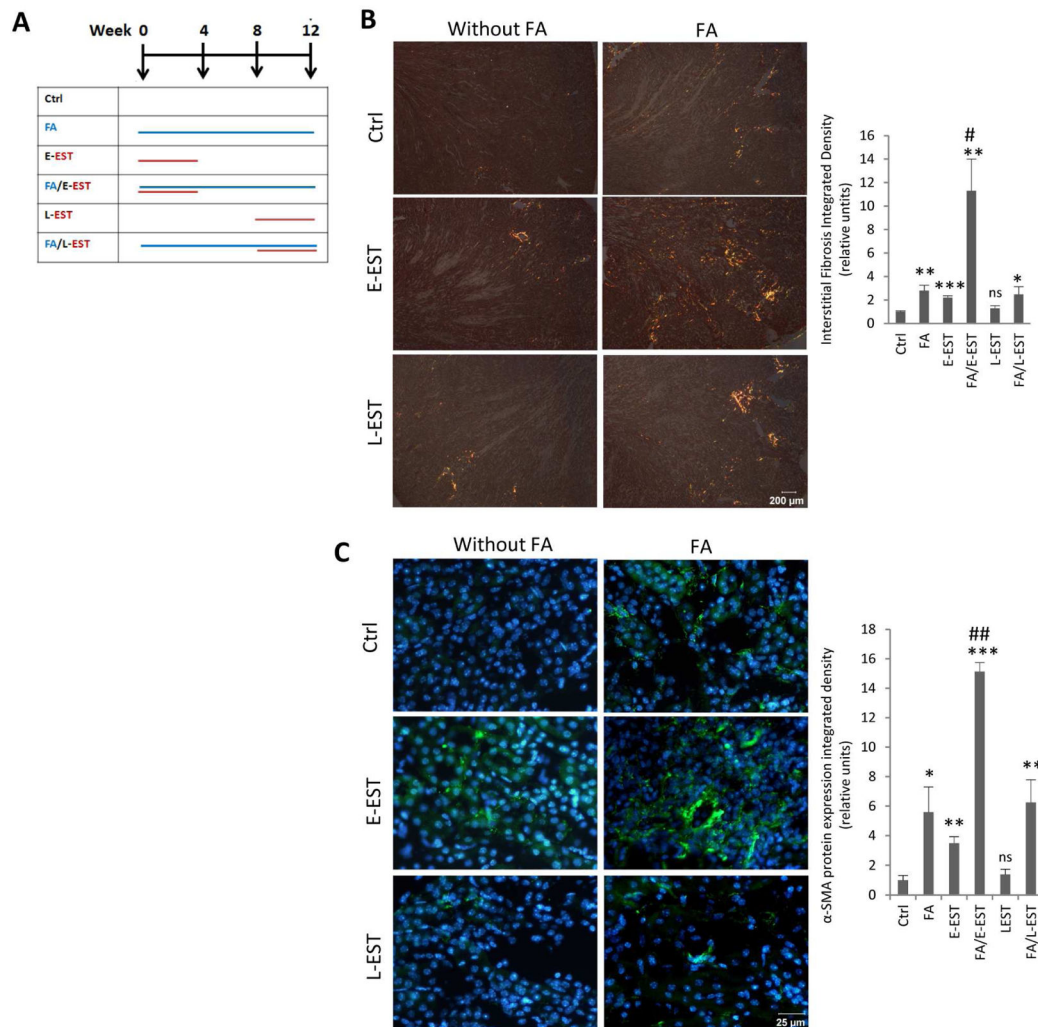


Fig 5. Interstitial fibrosis in mouse kidney after FA-induced nephropathy, with or without early or late EST peptide treatment

(A) Time course for the “second hit model” and EST delivery. When EST peptide delivering osmotic minipumps was implanted early during the course of FA-induced nephropathy (FA/E-EST group), the degree of fibrosis increased 11–14-fold compared with the control group as demonstrated by (B) Picosirius red staining and (C) α -SMA immunofluorescence staining. In contrast to FA/E-EST group, EST peptide minipumps implanted late into the disease failed to significantly change the degree of fibrosis occurring in FA-induced nephropathy (FA/L-EST group). Left panel: Representative images for each group are shown at magnification of $\times 400$. Right panel: (B) Quantification of integrated density using NIH image J at magnification of $\times 400$ and (C) quantification of results using grid method at magnification of $\times 400$. Data are means \pm SEM. *** $P < 0.001$ ** $P < 0.01$, * $P < 0.05$ compared with Ctrl group. ## $P < 0.01$, # $P < 0.05$ compared with Ctrl, E-EST, L-EST and FA/LEST groups. $n = 3-5$ animals per group.

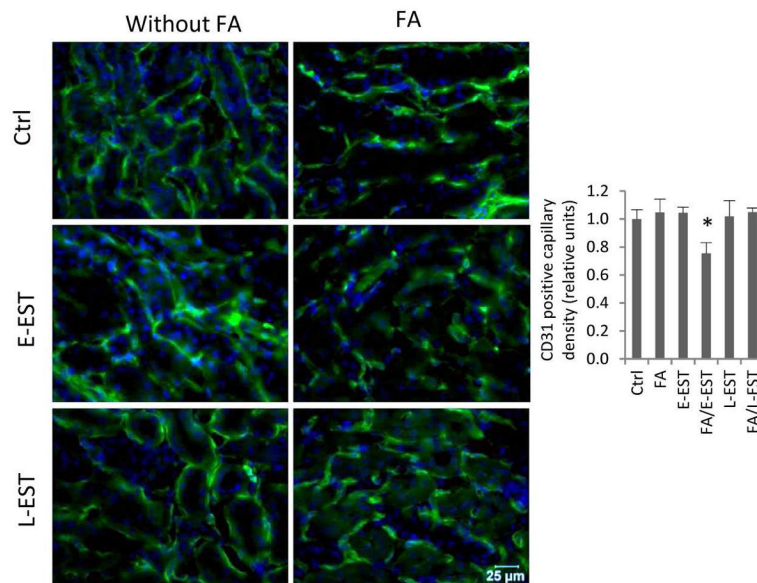


Fig 6. Renal peritubular capillary density in mouse kidneys after FA-induced nephropathy, with or without early or late EST peptide treatment
 Capillary density of the kidney cryo-sections showed a significant microvascular rarefaction in FA/E-EST group as reflected by the CD31 immunofluorescence staining. Left panel: Representative images for each group are shown at magnification of $\times 400$. Right panel: Quantification was performed using grid method. Data are means \pm SEM. $n=3-5$ animals per group. * $P<0.05$ compared to all other groups, except L-EST.

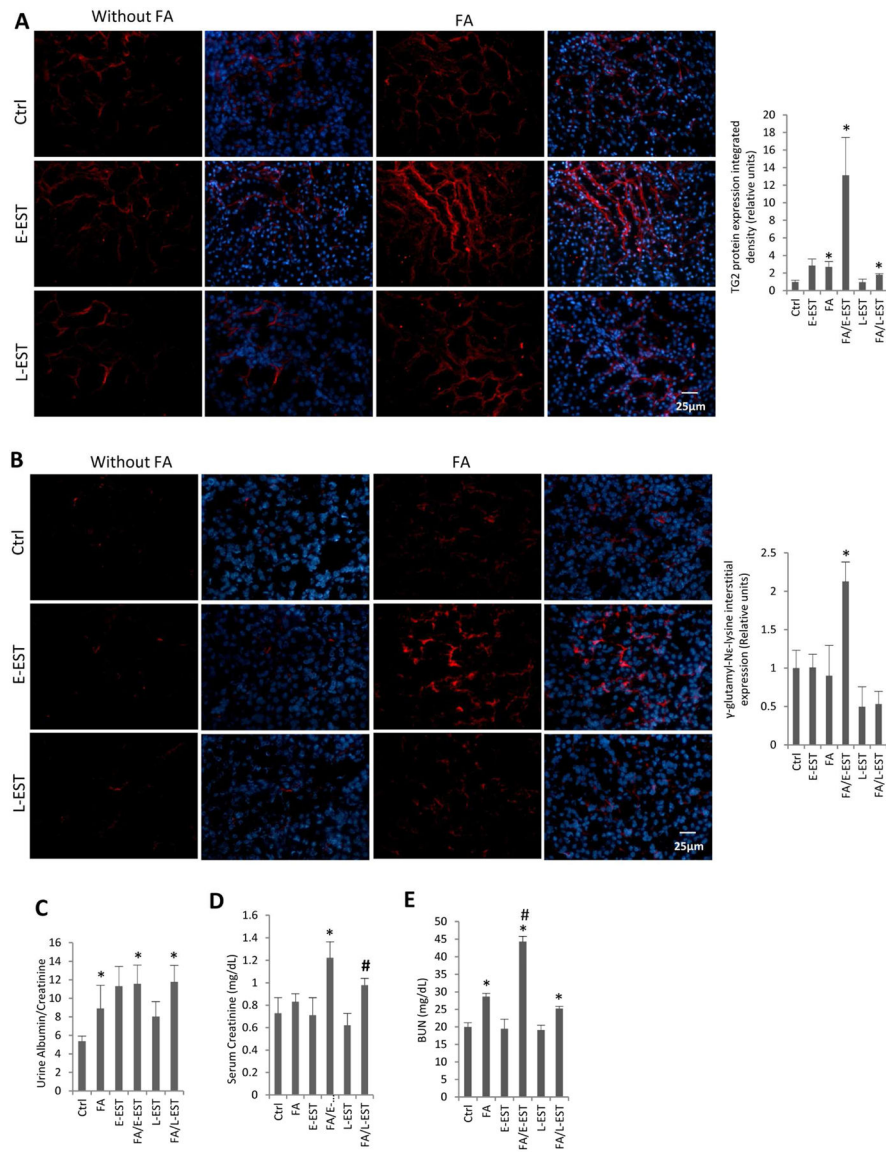


Fig 7. TG2 protein, cross-linking product γ -glutamyl-N^ε-lysine expression in mouse kidneys and kidney function after FA-induced nephropathy, with or without early or late EST peptide treatment

Immunofluorescence analyses of (A) TG2 and (B) the degree of cross-linking product γ -glutamyl-N^ε-lysine in the extracellular matrix increased significantly in the FA/E-EST group, but was not significantly changed in the FA/L-EST group. Left panel: Representative images at magnification of $\times 400$. Nuclear counterstaining was showed in the merged images. Right panel: Quantification of integrated density using image J. Data are means \pm SEM. * $P < 0.05$ compared with Ctrl. # $P < 0.05$ compared with all the other groups. $n = 3-5$ animals per group. (C, D and E) **Kidney function as determined by (C) urine albumin/creatinine ratio, (D) serum creatinine and (E) BUN after FA-induced nephropathy, with or without early or late EST peptide treatment.** Albuminuria (urine albumin/creatinine ratio), serum creatinine and BUN were measured 12 weeks after FA-induced nephropathy, with or without early or late EST peptide treatment for 4 weeks. Albuminuria,

serum creatinine and BUN were significantly elevated in mice of the FA/E-EST group, but changes were marginal in the FA/L-EST group. Data are mean \pm SEM. * $P < 0.05$ compared with control. # $P < 0.05$ compared with L-EST group (D), # $P < 0.05$ compared with FA and FA/L-EST group (E). $n = 3-5$ animals per group.

Author Manuscript

Author Manuscript

Author Manuscript

Author Manuscript

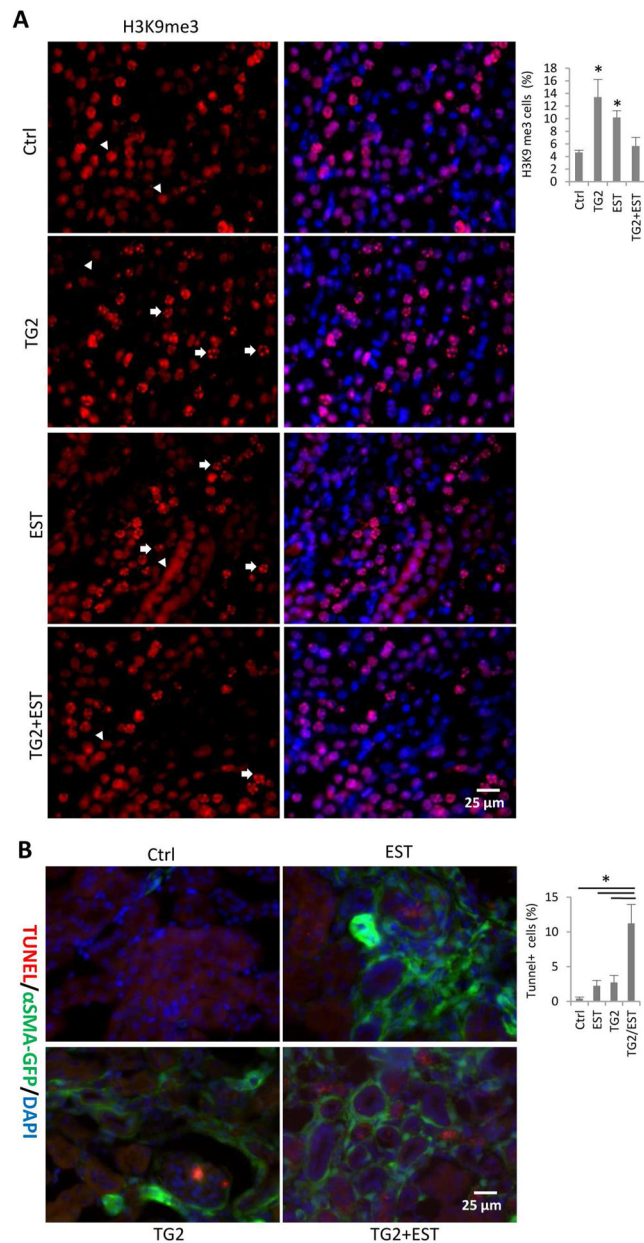


Fig 8. Senescence-associated heterochromatic foci (SAHF) H3K9me3 of kidneys injected with TG2 or EST

(A) 14 days after subcapsular lower pole injection with either buffer, or 2 ug of EST peptide, 1 ug of TG2 or TG2 plus EST dissolved in 10 μ l buffer. TG2 or EST injected mouse kidneys show increased H3K9Me3 staining. White arrow: Nucleus with enhanced accumulation of heterochromatin. White arrow head: Nucleus without enhanced accumulation of heterochromatin. Notably, combined injection of TG2 and EST did not show increased numbers of senescent cells. Right-hand panels depict merged images with the nuclear counterstaining. (B) In situ dead cell assay (TUNEL staining) of kidneys from the same groups showing a significantly increased number of labeled cells, some filled with the

apoptotic bodies, in TG2 and EST. Representative images for each group are shown at magnification of $\times 400$. Data are mean \pm SEM. * $P < 0.05$, $n = 3 \sim 4$ animals per group.

Author Manuscript

Author Manuscript

Author Manuscript

Author Manuscript

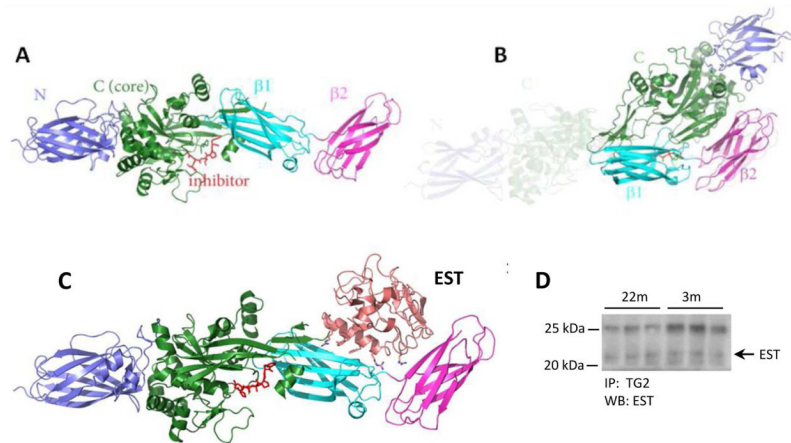


Fig 9. The ribbon model of TG2 and EST binding and Co-Immunoprecipitation of TG2 and EST (A) Open (active) conformation of TG2. The position of “inhibitor” highlights the active site of the enzyme. (B) Closed (inactive) conformation of TG2. The shaded area represents the former “open” conformation. (C) Model of EST binding to TG2 that leads to “freezing” TG2 in the open conformation. The position of EST denotes the mechanics of a forcible open conformation of TG2. It can also be postulated that the form of the enzyme lacking α - and β -barrels (the 53kDa fragment) should exhibit constitutively active catalytic site. (D) Kidney lysates (500 μ g proteins) were immunoprecipitated with anti-TG2 antibodies followed by immunoblotting with anti-EST antibodies. The predicted EST band is indicated by an arrow on the right. The upper band at position around 25 kDa is the IgG light chain.